# Chapter 10

# Optical detectors and Noise in Detection

#### 10.1 Optical detectors: The PMT <sup>1</sup>

The photomultiplier, one of the most common optical detectors, is used to measure radiation in the near ultraviolet, visible, and near infrared regions of the spectrum. Because of its inherent high current amplification and low noise, the photomultiplier is one of the most sensitive instruments devised by man and under optimal operation- which involves long integration time, cooling of the photocathode, and pulseheight discrimination-has been used to detect power levels as low as about  $10^{-19}$  watt.

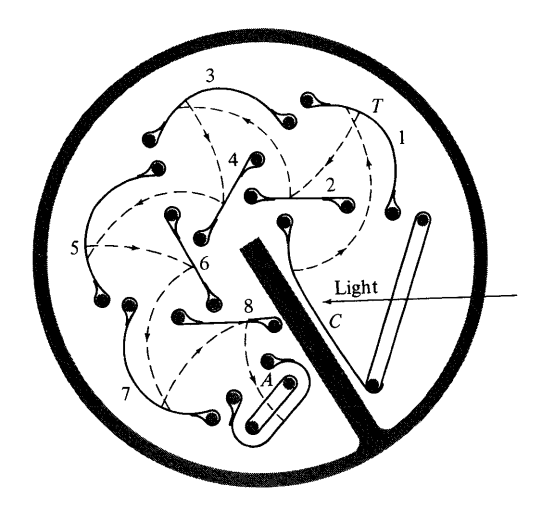


Figure 10.1: Photocathode and focusing dynode configuration of a typical commercial photomultiplier. C = cathode; 1-8 = secondary-emission dynodes; A = collecting anode.

A schematic diagram of a conventional photomultiplier is shown in Figure 10.1. It consists of a photocathode (C) and a series of electrodes, called dynodes, that' are labeled 1 through 8. The dynodes are kept at progressively higher potentials with respect to the cathode, with a typical potential difference between adjacent dynodes of 100 volts. The last electrode (A), the anode, is used to collect the electrons. The whole assembly is contained within a vacuum envelope in order to reduce the possibility of electronic collisions with gas molecules.

The photocathode is the most crucial part of the photomultiplier, since it converts the incident optical radiation to electronic current and thus determines the wavelength-response characteristics of the detector and, as will be seen, its limiting sensitivity. The photocathode consists of materials

 $<sup>^{1}</sup>$ Chapter 11 (Page 415 - 417) - Optical Electronics in Modern Communications- Fifth Edition - Amnon Yariv - Oxford University Press, 1997

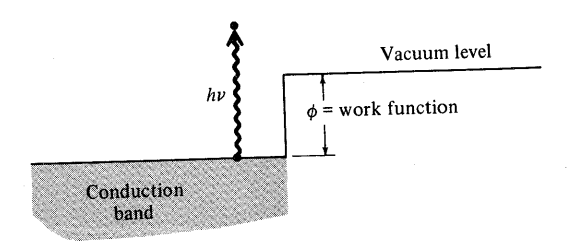
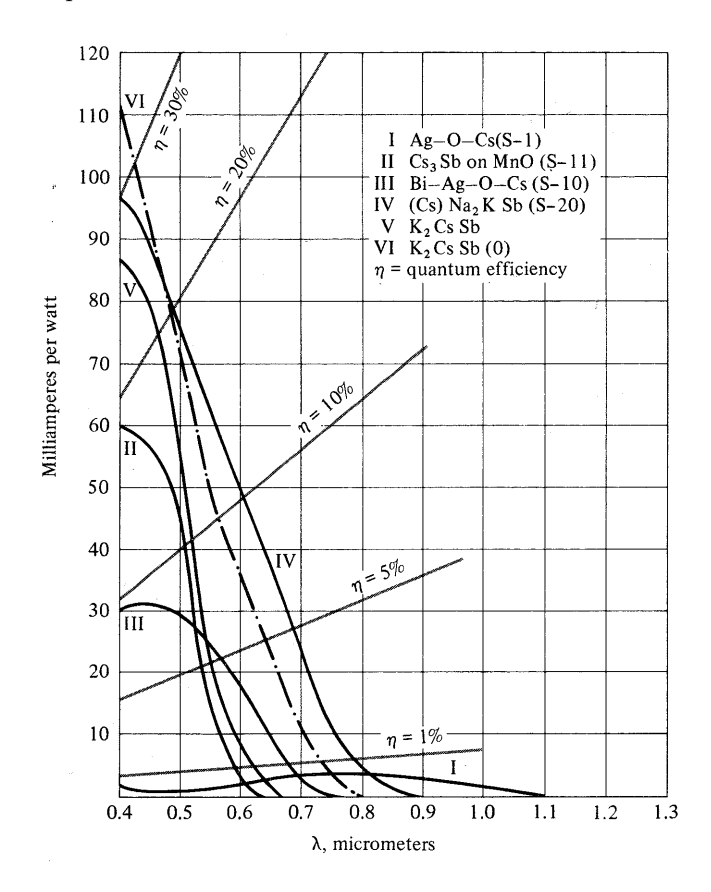


Figure 10.2: Photomultiplier photocathode. The vacuum level corresponds to the energy of an electron at rest at infinite distance from the cathode. The work function  $\phi$  is the minimum energy required to lift an electron from the metal into the vacuum level, so only photons with  $h\nu > \phi$  can be detected.

with low surface work functions. Compounds involving Ag-O-Cs and Sb-Cs are often used. These compounds possess work functions as low as 1.5 eV, as compared to 4.5 eV in typical metals. As can be seen in Figure 10.2, this makes it possible to detect photons with longer wavelengths. It follows from the figure that the low-frequency detection limit corresponds to  $h\nu = \phi$ . At present the lowest-work-function materials make possible photoemission at wavelengths as long as  $1 - 1.1\mu$ m.

Spectral response curves of a number of commercial photocathodes are shown in Figure 10.3. The quantum efficiency (or quantum yield as it is often called) is defined as the number of electrons released per incident photon.



**Figure 10.3:** Photoresponse versus wavelength characteristics and quantum efficiency of a number of commercial photocathodes.

The electrons that are emitted from the photocathode are focused electrostatically and accelerated toward the first dynode, arriving with a kinetic energy of, typically, about 100 eV. Secondary emission from dynode surfaces causes a multiplication of the initial current. This process repeats itself at each dynode until the initial current emitted by the photocathode is amplified by a very

large factor. If the average secondary emission multiplication at each dynode is  $\delta$  (that is,  $\delta$  secondary electrons for each incident one) and the number of dynodes is N, the total current multiplication between the cathode and anode is

$$G = \delta^N \tag{10.1.1}$$

which, for typical values <sup>2</sup> of  $\delta = 5$  and N = 9, gives  $G = 2 \times 10^6$ .

## 10.2 Optical detectors: Photodiode <sup>3</sup>

Semiconductor p-n junctions are used widely for optical detection. In this role they are referred to as junction photodiodes. The main physical mechanisms involved in junction photodetection are illustrated in Figure 10.4. At A, an incoming photon is absorbed in the p side creating a hole and a free electron. If this takes place within a diffusion length (the distance in which an excess minority concentration is reduced to  $e^{-1}$  of its peak value, or in physical terms, the average distance a minority carrier traverses before recombining with a carrier of the opposite type) of the depletion layer, the electron will, with high probability, reach the layer boundary and will drift under the field influence across it. An electron traversing the junction contributes a charge e to the current flow in the external circuit. If the photon is absorbed near then side of the depletion layer, as shown at C, the resulting hole will diffuse to the junction and then drift across it again, giving rise to a flow of charge e in the external load. The photon may also be absorbed in the depletion layer as at B, in which case both the hole and electron that are created drift (in opposite directions) under the field until they reach the p and n sides, respectively. Since in this case each carrier traverses a distance that is less than the full junction width, the contribution of this process to charge flow in the external circuit is e. In practice this last process is the most desirable, since each absorption gives rise to a charge e, and delayed current response caused by finite diffusion

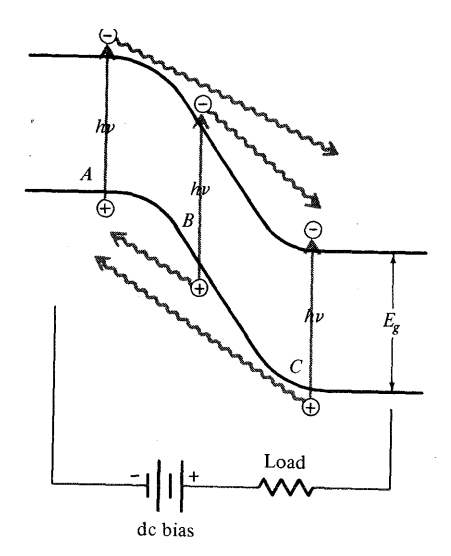


**Figure 10.4:** The three types of electron-hole pair creation by absorbed photons that contribute to current flow m a p-n photodiode..

time is avoided. As a result, photodiodes often use a p-i-n structure in which an intrinsic high resistivity (i) layer is sandwiched between the p and n regions. The potential drop occurs mostly across this layer, which can be made long enough to ensure that most of the incident photons are absorbed within It. Typical construction of a p-i-n photodiode is shown in Figure 10.5

It is clear from Figure (10.4) that a photodiode is capable of detecting only radiation With photon energy  $h\nu > E_q$ , where Egis the energy gap of the semiconductor. If, on the other

<sup>&</sup>lt;sup>2</sup>value of  $\delta$  depends on the voltage V between dynodes, and values of  $\delta \approx 10$  can be obtained (for  $V \approx 400$  volts). In commercial tubes, values of  $\delta = 5$  achievable with  $V \approx 100$  volts are commonly used.

 $<sup>^3</sup>$ Chapter 11 (Page 436- 438) - Optical Electronics in Modern Communications- Fifth Edition - Amnon Yariv - Oxford University Press, 1997

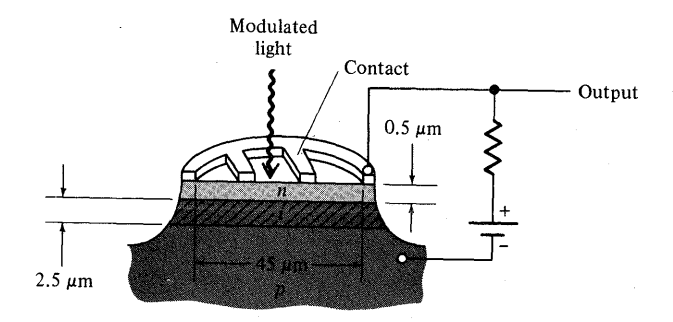


Figure 10.5: A p - i - n photodiode.

hand, $h\nu \gg E_g$ , the absorption, which in a semiconductor increases strongly with frequency, will take place entirely near the input face (in the n region of Figure 10.5) and the minority carriers generated by absorbed photons will recombine with majority carriers before diffusing to the depletion layer .. This event does not contribute to the current flow and, as far as the signal is concerned, is wasted. This is why the photoresponse of diodes drops off when  $h\nu > E_g$ . Typical frequency response curves of photodiodes are shown in Figure 10.6. The number of carriers flowing in the external circuit per incident photon, the so-called quantum efficiency, is seen to approach 50 percent in Ge.

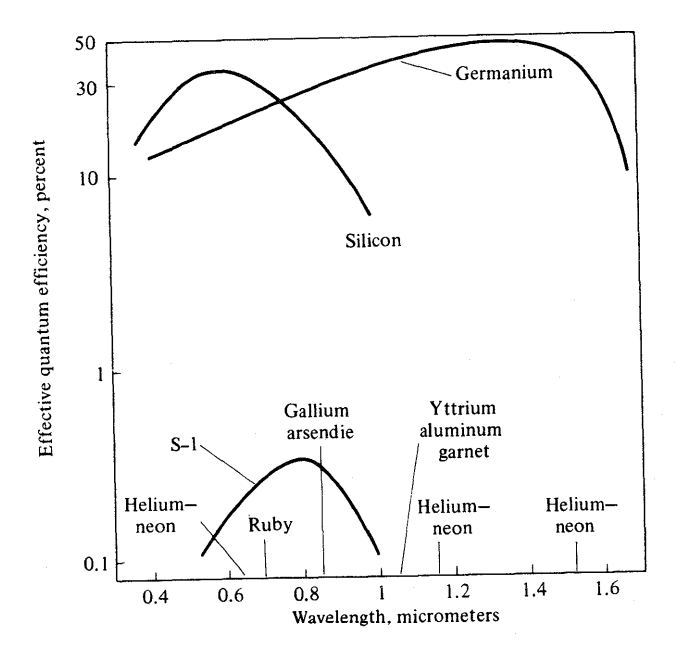


Figure 10.6: A p-i-n photodiode.

# 10.3 Optical detectors: The APD <sup>4</sup>

By increasing the reverse bias across a p-n junction, the field in the depletion layer can increase to a point at which carriers (electrons or holes) that are accelerated across the depletion layer can gain enough kinetic energy to "kick" new electrons from the valence to the conduction band, while still traversing the layer. This process, illustrated in Figure 10.7, is referred to as avalanche multiplication. An absorbed photon (A) creates an electron-hole pair. The electron is accelerated until at point C it has gained sufficient energy to excite an electron from the valence to the

 $<sup>^4</sup>$ Chapter 11 (Page 447- 448) - Optical Electronics in Modern Communications- Fifth Edition - Amnon Yariv - Oxford University Press, 1997

conduction band, thus creating a new electron-hole pair. The newly generated carriers drift in turn in opposite directions. The hole (F) can also cause carrier multiplication as in G. The result is a dramatic increase (avalanche) injunction current that sets in when the electric field becomes high enough. This effect, discovered first in gaseous plasmas and more recently in p-n junctions, gives

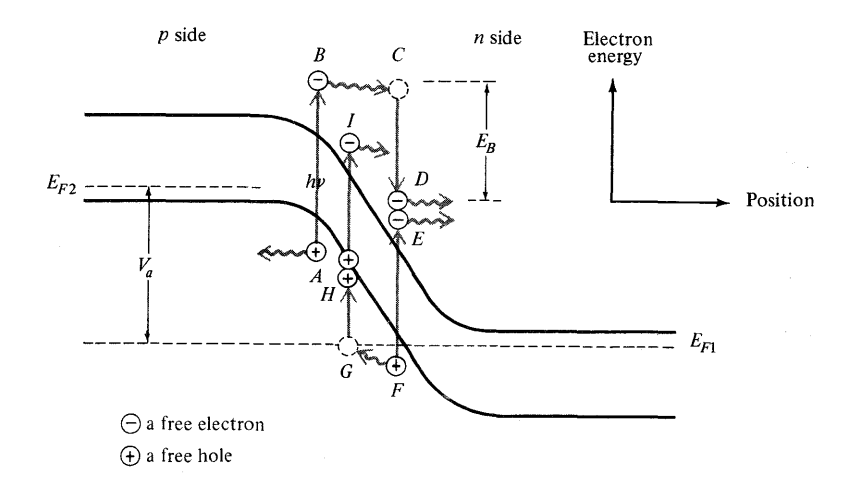


**Figure 10.7:** Energy-position diagram showing the carrier multiplication following a photon absorption in a reverse-biased avalanche photodiode.

rise to a multiplication of the current over its value in an ordinary (nonavalanching) photodiode. An experimental plot of the current gain M as a function of the junction field is shown in Figure 10.9.5

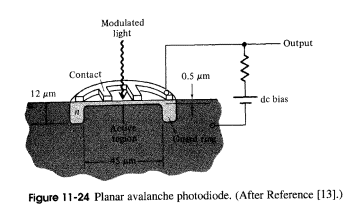


Figure 10.8: Planar avalanche photodiode.

Avalanche photodiodes are similar in their construction to ordinary photodiodes except that, because of the steep dependence of M on the applied field in the avalanche region, special care must be exercised to obtain very uniform junctions. A sketch of an avalanche photodiode is shown in Figure 10.8.

Since an avalanche photodiode is basically similar to a photodiode, its equivalent circuit elements are given by expressions similar to those given above for the photodiode. Its frequency response is similarly limited by diffusion, drift across the depletion layer, and capacitive loading.

A multiplication by a factor M of the photocurrent leads to an increase by  $M^2$  of the signal power S over that which is available from a photodiode so that, using , we get  $^6$ 

$$S \propto \overline{t_s^2} = 2M^2 \left(\frac{Pe\eta}{h\nu}\right) \tag{10.3.1}$$

 $<sup>^{5}</sup>$ If the probability that a photo-excited electron-hole pair will create another pair during its drift is denoted by p, the current multiplication is

 $M = (1 + p + p^2 + p^3 + \dots) = \frac{1}{1-p}$ 

 $<sup>^6</sup>$ A theoretical study by Mcintyre [17] predicts that if the multiplication is due to either holes or electrons, n = 2, whereas if both carriers are equally effective in producing electron-hole pairs, n = 3.

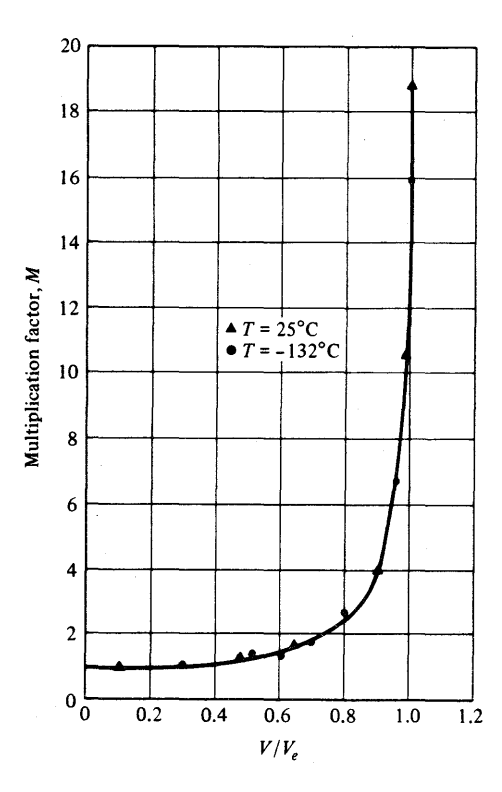


Figure 10.9: Current multiplication factor in an avalanche diode as a function of the electric field.

#### 10.4 Noise in optical detection<sup>7</sup>

This section discusses some of the dominant noise sources that limit the sensitivity in both coherent and direct-detection optical receiver configurations. Each noise source will be dealt with independently with the understanding that the total noise is found by summing the squares of the individual noise terms. For comparison purposes all noise sources will be referenced to the photodiode output current (see Figure 10.10). This reference position is a convenient location for the comparison of both optically and electrically generated noises. The photocurrent noise can be easily related to optical power sensitivity by use of the photodiode responsively, which is approximately 1 A/W at wavelengths around 1.55  $\mu$ m. Except for a change of units, the numerical values for photocurrent and optical power are almost identical. To provide a relatively easy way for comparing the magnitude of different noise sources, the concept of relative intensity noise (RIN) will be introduced. This describes noise as a fractional value, where the noise power in a 1 Hz bandwidth is normalized by the average power.

Each section will first give a general expression for describing the noise source. After this, examples will be given to illustrate how the expressions are used and to give a feeling for their magnitudes. For those who are interested, a simple derivation will be given near the end of each section. This derivation is not intended to be rigorous, but is hoped to provide a physical understanding for the process which generates the noise.

#### 10.5 Shot Noise and its derivation <sup>8</sup>

Electrical shot noise occurs because of the random arrival time of the electrons that make up an electrical current. It usually becomes an important noise source when trying to measure a small signal in the presence of a large DC background. This case normally occurs in coherent detection schemes where a small AC current is being measured in the presence of the large background due

<sup>&</sup>lt;sup>7</sup>Appendix A (597) - Fiber optic test and measurement - Derickson, Dennis- New Jersey: Prentice Hall, 1998
<sup>8</sup>Appendix A (605 - 607) - Fiber optic test and measurement - Derickson, Dennis- New Jersey: Prentice Hall, 1998

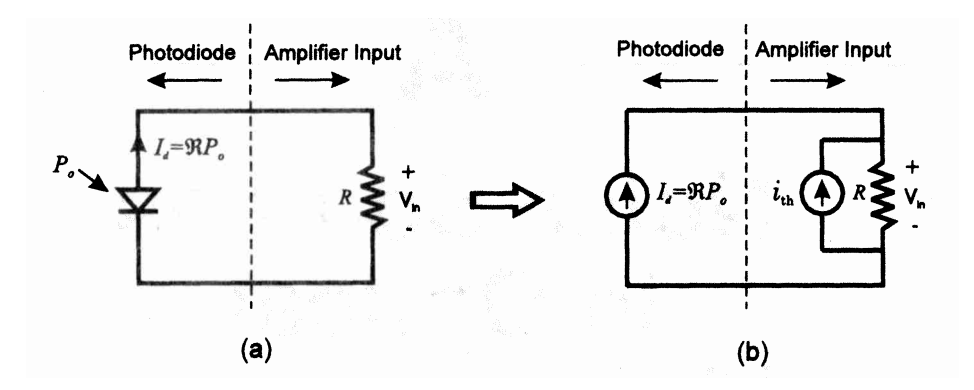


Figure 10.10: (a) Simplified Illustration of a photodiode connected to an electrical amplifier. (b) The equivalent circuit modeling the photodiode output and thermal resistive noise using Ideal current sources.

to the DC local oscillator current. The rms shot-noise current in a 1 Hz bandwidth is given by  $^9$ 

$$\hat{i}_{sn} = \sqrt{2qI_{dc}} \quad [A/\sqrt{Hz}]$$
 (10.5.2)

where  $q = 1.6 \times 10^{-19}$  C is the charge of an electron and  $I_{dc}$  is the DC photocurrent. Without frequency filtering, shot noise is spectrally flat and therefore has the above value at each measurement frequency. To calculate the total rms shot noise current  $(i_{sn})$  for an electrical circuit with an effective noise bandwidth  $(\Delta f)$ , Equation (10.5.2) should be multiplied by the square root of the bandwidth  $(i_{sn} = \hat{i}_{sn} \sqrt{\Delta f})$ .

An interesting observation can be made when comparing shot noise with thermal noise. Since the shot-noise level depends on signal current, there will be a point for increasing DC current when the shot-noise value exceeds the fixed thermal noise. It turns out that for a photodiode feeding into a resistor, the shot noise starts to exceed the thermal resistor noise when the voltage across the resistor becomes larger than 52 m V. This voltage level is independent of the value of the resistor. This result is useful in practice since it provides an easy method for determining which of the two noise sources is dominant. If the amplifying process generates excess noise, the value of 52 m V needs to be increased accordingly. Another point to mention is the special meaning that the shot-noise limit has in a coherent detection process. In this regime, the receiver has optimum sensitivity with a noise equivalent power equal to a single photon per integration time of the receiver.

Although RIN is defined as the fractional intensity noise on an optical signal, it can also be used in a nonconvential way to describe the level of shot noise on a dc photocurrent. By dividing the shot-noise current by the dc current and squaring the result, we get an expression equivalent to RIN. Expressing the shot noise this way, allows easy comparisons with other noise sources expressed in a similar manner. Using Equations A.5 and A.12, shot noise produces an effective RIN given by

$$RIN_{sn} = \frac{2q}{I_{dc}} [Hz^{-1}]$$
 (10.5.3)

This result is useful for determining the required dc photocurrent needed to make an accurate RIN measurement on an optical signal. The RIN<sub>sn</sub> decreases with dc photocurrent while the true optical RIN is independent of the dc signal. To make an accurate RIN measurement, one must ensure that a large enough dc photocurrent is detected to prevent shot noise from being the dominant noise source. For example, to measure a RIN of -155 dB/Hz on a DFB laser requires a photocurrent on the order of  $I_{dc} = 1mA$  or greater. Representative values of shot noise for different de photocurrents are shown in Table 11.1.

Simple derivation The following discussion shows a simple derivation for the shot-noise expression given in Equation (10.5.2). Shot noise can be thought of as being generated by the

$$S_I^{SN}(\omega) = 2qI_{DC} \qquad [A^2/Hz]$$
(10.5.1)

 $<sup>^9\</sup>mathrm{Hence}$  one can write the shot noise as a current spectral density

$I_{dc}$	$I_{sn}(pA/\sqrt{Hz})$	$RIN_{sn}(dB/Hz)$
100 nA	0.18	-115
$1 \mu A$	0.57	-125
$10 \ \mu A$	1.8	-135
$100 \ \mu A$	5.7	-145
1  mA	18	-155

Table 10.1: Representative shot-noise values.

random arrival time of electrons that make up a de photocurrent Figure 10.11 illustrates this random arrival-time process. Each vertical arrow represents the detection of a single particle at a specific time. In a nonrigorous manner these particles could also be photons. but for the purpose of this derivation they will be assumed to be electrons. The above random arrival time can be described by a Poisson probability process. This type of process has the characteristic that in any given time interval. the variance (or rms uncertainty) in the number of electrons is equal to the square root of the average number.

$$\Delta N_{rms} = \sqrt{\overline{N}} \tag{10.5.4}$$

This variation in the average number of arriving electrons during any specified time interval leads to the generation of shot-noise. The rms shot noise current can be written as the rms variation in detected charge per unit time as

$$i_{sn} = \frac{q\Delta N_{rms}}{\Delta t} \quad [A] \tag{10.5.5}$$

where q is the charge of the electron and  $\Delta t$  is the measurement time interval. The dc photocurrent can be expressed in a similar manner using the average number of electrons per time interval as

$$I_{dc} = \frac{q\bar{N}}{\Delta t} \quad [A] \tag{10.5.6}$$

This result allows us to express the rms shot noise current in terms of the dc current using the

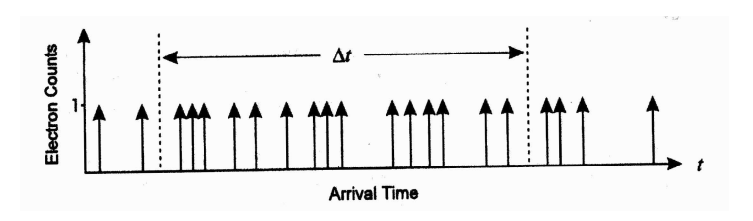


Figure 10.11: Random arrival time of photogenerated electrons.

above three equations.

$$i_{sn} = \sqrt{\frac{qI_{dc}}{\Delta t}} \quad [A] \tag{10.5.7}$$

To put this expression into a more commonly used form, we must relate the measurement time interval to an equivalent noise bandwidth. Using Fourier analysis it can be shown that the effective noise bandwidth  $\Delta f$  of a flat-topped rectangular gate function of width  $\Delta t$  is given by

$$\Delta f = \frac{1}{2\Delta t} \quad [Hz] \tag{10.5.8}$$

With this result we can now convert Equation (10.5.7) into the familiar expression

$$i_{sn} = \sqrt{2qI_{dc}\Delta f} \quad [A]$$
 (10.5.9)

which is equivalent to the result given in Equation (10.5.2).

An equivalent argument can be made for the shot-noise intensity on an optical signal by considering photons instead of electrons. Now the random arrival time of the photons leads to a

fluctuation in the optical power. For this situation. the above equations can be rewritten by replacing the electrical charge with the photon energy  $(q \to h\nu)$  and the current with the optical power  $(I_{dc} \to P_{cw})$ . When using this classical concept to describe photons, care must be used since it is not rigorous in a quantum mechanical sense and can lead to incorrect results.

Squeezed States As a final comment on shot-noise. an attempt will be made to describe the concept of optical squeezed states. Squeezed states is a quantum mechanical concept describing the reduction in the "optical shot-noise" on a cw optical signal. Or in other words, removing the randomness in the arrival time (see Figure 10.11) of photons and thereby decreasing the associated optical intensity noise. Squeezed states makes use of the uncertainty principle between the position and momentum (in other words, frequency) of a photon. The uncertainty in the photon position can be reduced at the expense of increasing the uncertainty in the photon frequency.

This concept can be understood by replacing the electrons in Figure A.4 with photons. This can be rationalized since for the case of a 100% quantum efficiency detector, there is a one-to-one correspondence between the input photons and the generated electrons. By producing a more equal spacing between photons, the intensity noise is reduced since the uncertainty in the number of photons in a given measurement time becomes less than  $\sqrt{N}$ . The process of "squeezing" the intensity fluctuations out of an optical signal requires that the positions of the individual photons become well defined. Due to the uncertainty principle, this increases the uncertainty of the photon frequency (or momentum) which leads to a broadening of the optical bandwidth. The more the intensity noise is reduced the larger the optical bandwidth becomes. Although squeezed states have been demonstrated experimentally, reducing the shot noise by more than a several dB becomes extremely difficult.

## 10.6 Johnson Noise <sup>10</sup>

One common noise source, which needs to be considered in almost every detection process, is the thermal noise generated in the receiver electronics. If the receiver amplifying process is considered ideal, so that no excess noise is generated, the resulting receiver noise will be determined by the thermal noise (also known as Johnson noise) generated by the resistance first experienced by the photocurrent. As this resistance is made larger the optical power sensitivity is improved. This result will become more evident in the following discussions.

Thermal noise from a resistor can be modeled as being generated by either a voltage or current noise source. Since the signal from a photodiode looks as if it were generated by a current source, it is more convenient to use the current noise-source model for describing thermal noise. This allows the current noise to be directly .compared to the generated photocurrent.

Figure 10.10a shows the basic configuration for generating. a signal voltage using a photodiode and external resistor. Figure 10.10b is a simplified equivalent circuit which uses current sources to model the photodiode and thermal noise generated by the resistor. For simplicity the circuit capacitances have been omitted, but they would need to be included for determining the effective noise bandwidth of the circuit. As modeled in Figure 10.10 b, the thermally generated rms current noise  $\hat{i}_{th}$  in a 1 Hz bandwidth is given by<sup>11</sup>

$$\left| \hat{i}_{th} = \sqrt{\frac{4kT}{R}} \quad [A/\sqrt{Hz}] \right| \tag{10.6.2}$$

where R is the resistance which the photocurrent first experiences,  $k = I.38 \times 10^{-23} \text{J/K}$  is Boltzman's constant and T is the temperature of the resistor in Kelvin. The caret above the rms current symbol is used to indicate that the current noise is normalized to a 1Hz bandwidth. This normalized expression is useful when comparing the magnitude of the thermal noise with the other

$$S_I^{TN}(\omega) = \frac{4k_BT}{R} \qquad [A^2/Hz]$$
(10.6.1)

(added by authors)

<sup>10</sup> Appendix A (598 - 599) - Fiber optic test and measurement - Derickson, Dennis- New Jersey : Prentice Hall,

 $<sup>^{11}</sup>$ Hence one can write the thermal noise via the spectral density of current fluctuations as:

noise sources in the system. The total rms current  $(i_{th})$  noise is obtained by multiplying Equation (10.6.2) by the square root of the receiver bandwidth  $(i_{th} = \hat{i}_{th}\sqrt{\Delta f})$ .

As seen from Equation (10.6.2), the thermal current noise (or optical power sensitivity) is reduced by making the resistance larger. This is the opposite result when considering standard, voltage-based electronic circuits. Although a larger resistor reduces receiver noise, the actual value used is usually a compromise between sensitivity and receiver bandwidth. It should be pointed out that for a trans-impedance receiver, the resistance in Equation (10.6.2) is the feedback resistance and not the effective input impedance seen by the photodiode.

In practice, the actual noise at the output of the amplifier will be larger due to the excess noise added in the amplifying process. But Equation (10.6.2) is still useful since it predicts the best possible performance given a specific receiver impedance. The room temperature  $(T \sim 300K)$  current noise for some representative values of receiver resistance are given in Table A.I

$\overline{I_{dc}}$	$I_{sn}(pA/\sqrt{Hz})$	$RIN_{sn}(dB/Hz)$
$\frac{100 \text{ nA}}{100 \text{ nA}}$	$\frac{1sn(P17,V113)}{0.18}$	$\frac{1011 \cdot \sin(\sin(\pi D/11 \pi))}{-115}$
$1 \mu A$	0.57	-125
$10 \ \mu A$	1.8	-135
$100 \ \mu A$	5.7	-145
1 mA	18	-155

Table 10.2: Representative shot-noise values.

#### 10.7 Statistical derivation of the Johnson Noise 12

The derivation of Johnson noise leans heavily on thermodynamic and statistical mechanics considerations. It may be instructive to obtain this result using a physical model for a resistance and applying the mathematical tools developed in this chapter. The model used is shown in Figure 10.12.

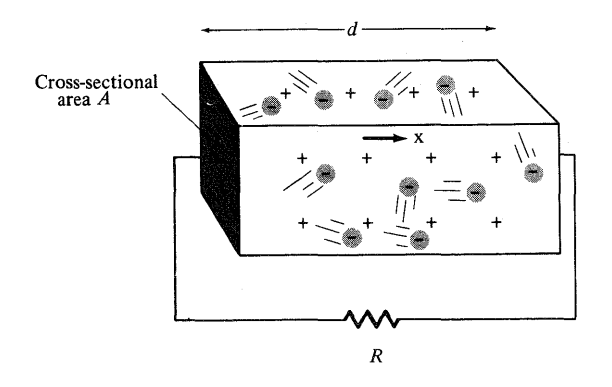


Figure 10.12: Model of a resistance used in deriving the Johnson-noise formula.

The resistor consists of a medium of volume V = Ad, which contains  $N_e$  free electrons per unit volume. In addition, there are  $N_e$  positively charged ions, which preserve the (average) charge neutrality. The electrons move about randomly with an average kinetic energy per electron of

$$\overline{E} = \frac{3}{2}kT = \frac{1}{2}m(\overline{v_x^2} + \overline{v_y^2} + \overline{v_z^2}) \tag{10.7.1}$$

where  $\overline{v_x^2} = \overline{v_y^2} = \overline{v_z^2}$  refer to thermal averages. A variety of scattering mechanisms X y Z including electron-electron, electron-ion, and electron-phonon collisions act to interrupt the electron motion

 $<sup>^{12}{\</sup>rm Chapter}$  10 (Page 386-388) - Optical Electronics in Modern Communications- Fifth Edition - Amnon Yariv - Oxford University Press, 1997

at an average rate of  $\tau_0^{-1}$  times per second.  $\tau_0$  is thus the mean scattering time. These scattering mechanisms are responsible for the electrical resistance and give rise to a de conductivit.<sup>13</sup>

$$\sigma = \frac{N_e e^2 \tau_0}{m} \tag{10.7.2}$$

where m is the mass of the electron. The sample de resistance is thus

$$R = \frac{d}{\sigma A} = \frac{md}{Ne^2 \tau_0 A} \tag{10.7.3}$$

while its ac resistance  $R(\omega)$  is  $md(1+\omega^2\tau_0^2)/Ne^2\tau_0A$ .

We choose as our basic single event the current pulse  $i_e(t)$  in the external circuit due to the motion of one electron between two successive scattering events. Using

$$i_e(t) = \frac{ev(t)}{d} \tag{10.7.4}$$

where v(t) is the speed of the electron and d is the separation of end plates (Figure 10.12), we can write:

$$i_e(t) = \begin{cases} \frac{ev_x}{d} & 0 \le t \le \tau \\ 0 & \text{otherwise} \end{cases}$$
 (10.7.5)

where  $v_x$  is the x component of the velocity (assumed constant) and where  $\tau$  is the scattering time of the electron under observation. Taking the Fourier transform of  $i_e(t)$ , we have

$$I_{e}(\omega, \tau, v_{x}) = \frac{1}{2\pi} \int_{0}^{\tau} i_{e}(t)e^{-i\omega t}dt = \frac{(1/2\pi)ev_{x}}{-i\omega d}[e^{-i\omega\tau} - 1]$$
 (10.7.6)

from which

$$|I_e(\omega, \tau, v_x)|^2 = \frac{e^2 v_x^2}{4\pi^2 \omega^2 d^2} [2 - e^{i\omega\tau} - e^{-i\omega\tau}]$$
(10.7.7)

In the next step we need to average  $|I_e(\omega, \tau, v_x)|^2$  over the parameters  $\tau$  and  $v_x$ . We assume that  $\tau$  and  $v_x$  are independent variables - that is, that the probability function

$$p(\alpha) = p(\tau, v_x) = g(\tau)f(v_x) \tag{10.7.8}$$

is the product of the individual probabilities - and take  $g(\tau)$  as 15

$$g(t) = \frac{1}{\tau_0} e^{-t/\tau} \tag{10.7.10}$$

and, performing the average over  $\tau$ , obtain

$$\overline{|I_e(\omega, v_x)|^2} = \int_0^\infty g(\tau) |I_e(\omega, \tau, v_x)|^2 d\tau = \frac{2e^2 v_x^2 \tau_0^2}{4\pi^2 d^2 (1 + \omega^2 \tau_0^2)}$$
(10.7.11)

$$q'(t) = -q(t)\frac{1}{\tau_0} \implies q(t) = e^{-t/\tau_0}$$

Taking g(t)dt as the probability that a collision will occur between  $\tau$  and t+dt, it follows that

$$q(t) = 1 - \int_0^t g(t')dt'$$

and thus

$$g(t) = -\frac{dq}{dt} = \frac{1}{\tau_0} e^{-t/\tau} \tag{10.7.9}$$

as in (10.7.10).

<sup>&</sup>lt;sup>13</sup>The derivation of (10.7.2) can be found in any introductory book on solid-state physics.

<sup>&</sup>lt;sup>14</sup>In a semiconductor we use the effective mass of the charge carrier.

<sup>&</sup>lt;sup>15</sup> If the collision probability per carrier per unit times is  $1/\tau_0$  and q(t) is the probability that an electron has not collided by time t, we have:

The second averaging over  $v_x^2$  is particularly simple, since it results in the replacement of  $v_x^2$  in (10.7.11) by its average  $v_x^2$ , which, for a sample at thermal equilibrium, is given according to (10.7.1) by  $v_x^2 = kT/m$ . The final result is then

$$\overline{|I_e(\omega)|^2} = \frac{2e^2\tau_0^2kT}{4\pi^2md^2(1+\omega^2\tau_0^2)}$$
(10.7.12)

The average number of scattering events per second  $\overline{N}$  is equal to the total number of electrons  $N_eV$  divided by the mean scattering time  $\tau_0$ 

$$\overline{N} = \frac{N_e V}{\tau_0} \tag{10.7.13}$$

thus we obtain

$$S_i(\nu) = 8\pi^2 \overline{N} |I_e(\omega)|^2 = \frac{4NVe^2 \tau_0 kT}{md^2 (1 + \omega^2 \tau_0^2)}$$
(10.7.14)

and, after using (10.7.3) and limiting ourselves as to frequencies where  $\omega \tau_0 \ll 1$ , we get

$$\boxed{\overline{i_N^2}(\nu) \equiv S_i(\nu)\Delta\nu = \frac{4kT\Delta\nu}{R(\nu)}}$$
(10.7.15)

#### 10.8 Direct detection and total noise on a photodiode <sup>16</sup>

The three noise sources studied in this appendix represent the most common noise sources associated with optical detection. For simplicity, each noise source was considered separately. In real situations, all the individual noise sources need to be combined to determine the total noise level for the detection system. Since the above noises are uncorrelated with each other, the total rms photocurrent noise  $(i_{\text{tolal}})$  is given by summing their squares and then taking the square root. This procedure is shown analytically as

$$i_{\text{total}} = \sqrt{\frac{4kT\Delta f}{R} + 2qI_{dc}\Delta f + I_{dc}^2 \text{RIN}\Delta f}$$
(thermal) (shot) (intensity)

where the definitions of the parameters can be found in the previous four sections. To keep the expression simple, each noise term is assumed spectrally flat over the bandwidth  $\Delta f$  If this is not the case, a separate integration over frequency would be required for each term under the square root sign.

Figure (10.13) shows the graphical result of combining several of the above noise sources for a high-speed communications receiver. The receiver consists of a room temperature reversed-biased pin photodetector connected to a load impedance of  $1K\Omega$ .

To reduce the complexity of the example, the amplification of the photocurrent is assumed ideal so all of the post-detection noise is generated by the thermal noise of the  $1K\Omega$  load resistance. Only the first three noise terms (thermal, shot, and intensity) in Equation (10.8.1) are considered. The optical source is assumed to be a DFB laser with a RIN of -155 dB/Hz. Figure (10.13) shows the rms current noise in a 1 Hz bandwidth, as a function of the dc photocurrent. Each of the three noise terms are plotted separately along with the total noise as computed using Equation (10.8.1). For low power levels ( $I_{dc} < 52\mu$ A) the noise is dominated by the thermal noise of the load impedance. For dc currents between  $52\mu$ A and 1 mA, the shot noise dominates. And for currents in excess of 1 mA the intensity noise from the DFB source is dominant.

The sensitivity of the receiver to optical power changes can be determined using the total noise current given by Equation (10.8.1). This is simply calculated using

$$\Delta P_{min} = \frac{i_{\text{total}}}{\Re} \quad [W] \tag{10.8.2}$$

where  $\Re$ . represents the responsively (in units amps/watts) of the photodiode. This minimum power sensitivity depends on the square root of the detection bandwidth as shown in Equation (10.8.1).

 $<sup>^{16}\</sup>mathrm{Appendix}$  A (612-613) - Fiber optic test and measurement - Derickson, Dennis- New Jersey : Prentice Hall, 1998

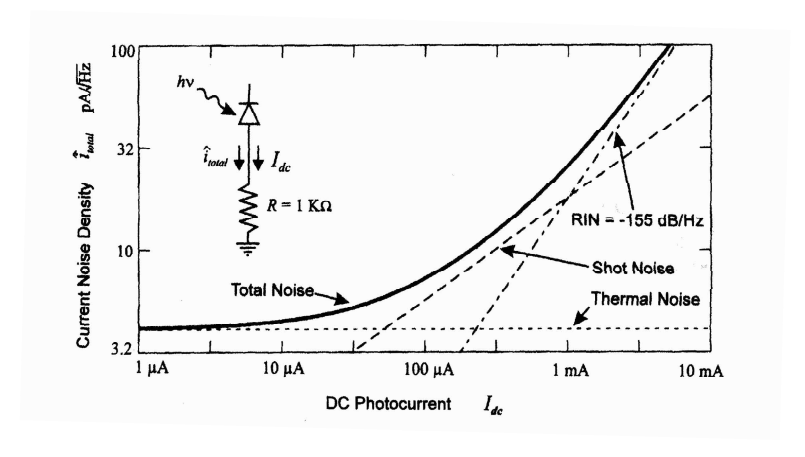


Figure 10.13: Total rms photocurrent noise normalized to a 1Hz bandwidth. caused by the combined effects of thermal, shot, and Intensity noise.

#### Example: Sensitivity of a receiver

This example determines the sensitivity of a receiver in the presence of a large dc optical power. Consider the case of a reverse-biased photodiode connected to an electrical circuit with an effective noise bandwidth of 500 MHz. Suppose the incident optical power is  $P_o$ = 1.25 mW and the resulting photocurrent is  $I_{dc}=1.0$  mA. From these values the photodiode responsively is calculated to be  $\Re=I_{dc}/P_a=0.8$  A/W. Assuming that the dominant noise source is the shot noise from the 1 mA dc current. Table 11.1 gives a rms noise current density of 18 pA/ $\sqrt{\rm Hz}$ . Multiplying this value by the square root of the noise bandwidth gives a total rms current noise of  $i_{\rm total}=0.4\mu{\rm A}$ . Equation (10.8.2) can now be used to calculate a receiver sensitivity of 0.5  $\mu{\rm W}$ . This sensitivity corresponds to a modulation depth in the input power of  $4\times 10^{-4}$ .

## 10.9 Heterodyne detection <sup>17</sup>

In the heterodyne mode of optical detection, the signal to be detected  $E_s \cos \omega_s t$  is combined with a second optical field, referred to as the local-oscillator field,  $E_L \cos(\omega_s + \omega)t$ , shifted in frequency by  $\omega(\omega \ll \omega_s)$ . The total field incident on the photocathode is therefore given by

$$e(t) = Re[E_L e^{i(\omega_s + \omega)t} + E_s e^{i\omega_s t}] \equiv Re[V(t)]$$
(10.9.1)

The local-oscillator field originates usually at a laser at the receiving end, so that it can be made very large compared to the signal to be detected. In the following we will assume that

$$E_L \gg E_s \tag{10.9.2}$$

A schematic diagram of a heterodyne detection scheme is shown in Figure 11-6. The current emitted by the photocathode is given, according to (10.9.1), by

$$i_c(t) \propto V(t)V^*(t) = E_L^2 + E_s^2 + 2E_L E_s \cos \omega t$$
 (10.9.3)

which, using (10.9.2) can be written as

$$i_c(t) = aE^2 \left( 1 + \frac{2E_s}{E_L} \cos(\omega t) \right) = aE_L^2 \left( 1 + 2\sqrt{\frac{P_s}{P_L}} \cos(\omega t) \right)$$
 (10.9.4)

 $<sup>^{17}\</sup>mathrm{Chapter}$ 11 (Page 421-424) - Optical Electronics in Modern Communications- Fifth Edition - Amnon Yariv - Oxford University Press, 1997

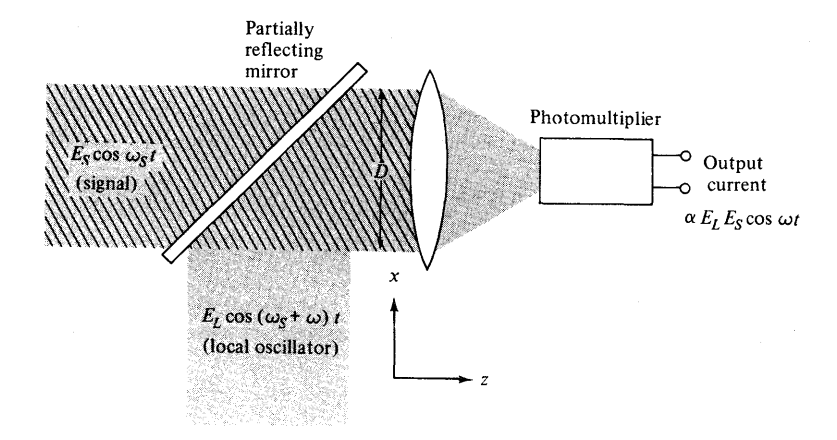


Figure 10.14: Schematic diagram of a heterodyne detector using a photomultiplier.

where  $P_s$  and  $P_L$  are the signal and local-oscillator powers, respectively. The proportionality constant a in (10.9.4) can be determined by requiring that when  $E_s=0$  the direct current be related to the local-oscillator power  $P_L$  by  $\overline{i}_c=P_L\eta e/h\nu_L^{-18}$  so taking  $\nu\approx\nu_L\approx\nu_s$ 

$$i_c(t) = \frac{P_L e \eta}{h \nu} \left( 1 + 2 \sqrt{\frac{P_s}{P_L}} \cos(\omega t) \right)$$
 (10.9.5)

The total cathode shot noise is thus

$$\overline{(i_{N_1}^2)} = 2e\left(i_d + \frac{P_L e\eta}{h\nu}\right) \Delta\nu$$
(10.9.6)

where  $i_d$  is the average dark current while  $P_L$  by  $\overline{i}_c = P_L \eta e/h\nu_L$  is the de cathode current due to the strong local-oscillator field. The shot-noise current is amplified by G, resulting in an output noise

$$\overline{(i_N^2)}_{\text{anode}} = G^2 2e \left( i_d + \frac{P_L e \eta}{h \nu} \right) \Delta \nu \tag{10.9.7}$$

The mean-square signal current at the output is, according to (10.9.5).

$$\overline{(i_s^2)}_{\text{anode}} = G^2 2e \left(\frac{P_s}{P_L}\right) \left(\frac{P_L e \eta}{h \nu}\right)^2$$
(10.9.8)

The signal-to-noise power ratio at the output is given by

$$\frac{S}{N} = \frac{2G^2(P_s P_L)(e\eta/h\nu)^2}{[G^2 2e(i_d + P_L e\eta/h\nu) + 4kT_e/R]\Delta\nu}$$
(10.9.9)

where the last term in the denominator, represents the Johnson (thermal) noise generated in the output load. plus the effective input noise of the amplifier following the photomultiplier The big advantage of The heterodyne detection scheme is now apparent. By increasing  $P_L$  the S/N ratio increases until the denominator is dominated by the term  $G^2 2eP_L e\eta/h\nu$ . This corresponds to the point at which the shot noise produced by the local oscillator current dwarfs all her other noise contriburtion. When this state of affairs prevails, we have, according to (10.9.9),

$$\boxed{\frac{S}{N} \simeq \frac{P_s}{h\nu\Delta\nu/\eta}} \tag{10.9.10}$$

 $<sup>^{18}</sup>$ This is just a statement of the fact that each incident photon has a probability  $\eta$  of releasing an electron

which corresponds to the quantum - limited detection limit. The minimum detectable signal - that is, the signal input power leading to an output signal-to-noise ratio of 1- is thus

$$(P_s)_{min} = \frac{h\nu\Delta\nu}{\eta}$$
(10.9.11)

This power corresponds for  $\eta = 1$  to a flux at a rate of one photon per  $(\Delta \nu)^{-1}$  seconds-that is, one photon per resolution time of the system. <sup>19</sup>

#### Limiting Sensitivity as a Result of the Particle Nature of Light

The quantum limit to optical detection sensitivity is given by (10.9.11) as

$$(P_s)_{min} = \frac{h\nu\Delta\nu}{\eta} \tag{10.9.12}$$

This limit was shown to be due to the shot noise of the photoemitted current. We may alternatively attribute this noise to the granularity-that is, the particle nature - of light, according to which the minimum energy increment of an electromagnetic wave at frequency  $\nu$  is  $h\nu$ . The average power P of an optical wave can be written as

$$P = \overline{N}h\nu \tag{10.9.13}$$

where  $\overline{N}$  is the average number of photons arriving at the photocathode per second. Next assume a hypothetical noiseless photomultiplier in which *exactly* one electron is produced for each  $\eta^{-1}$  incident photons. The measurement of P is performed by counting the number of electrons produced during an observation period T and then averaging the result over a large number of similar observations.

The average number of electrons emitted per observation period T is

$$\overline{N}_e = \overline{N}T\eta \tag{10.9.14}$$

If the photons arrive in a perfectly random manner, then the number of photons arriving during the fixed observation period obeys Poissonian statistics.<sup>20</sup> Since in our ideal example, the electrons that are emitted mimic the arriving photons, they obey the same statistical distribution law. This leads to a fluctuation

$$\overline{(\Delta N_e)^2} \equiv \overline{(N_e - \overline{N_e})^2} = \overline{N_e} = \overline{N}T\eta \tag{10.9.18}$$

Defining the minimum detectable number of quanta as that for which the rms fluctuation in the number of emitted photoelectrons equals the average value, we get

$$(\overline{N}_{min}T\eta)^{1/2} = \overline{N}_{min}T\eta \tag{10.9.19}$$

or

$$(\overline{N})_{min} = \frac{1}{T\eta} \tag{10.9.20}$$

$$p(N) = \frac{(\overline{N})^N e^{-\overline{N}}}{N!}$$
(10.9.15)

The mean-square fluctuation is given by

$$\overline{(\Delta N)^2} = \sum_{N=0}^{\infty} p(N)(N - \overline{N})^2 = \overline{N}$$
(10.9.16)

where

$$\overline{N} = \sum_{N=0}^{\infty} Np(N) \tag{10.9.17}$$

is the average N.

<sup>&</sup>lt;sup>19</sup>A detection system that is limited in bandwidth to  $\Delta\nu$  cannot resolve events in time that are separated by less than  $(\Delta\nu)^{-1}$  second. Thus  $(\Delta\nu)^{-1}$  is the resolution time of the system.

 $<sup>^{20}</sup>$ This follows from the assumption that the photon arrival is perfectly random, so the probability of having N photons arriving in a given time interval is given by the Poisson law

If we convert the last result to power by multiplying it by  $h\nu$  and recall that  $T^{-1} \simeq \Delta\nu$ , where  $\Delta\nu$  is the bandwidth of the system, we get

$$(P_s)_{min} = \frac{h\nu\Delta\nu}{\eta} \tag{10.9.21}$$

The above discussion points to the fact that the noise (fluctuation) in the photo current can be blamed on the physical process that introduces the randomness. In the case of Poissonian photon arrival statistics (as is the case with ordinary lasers) and perfect photon emission ( $\eta=1$ ), the fluctuations are due to the photons. The opposite, hypothetical, case of no photon fluctuations but random photoemission ( $\eta<1$ ) corresponds to pure shot noise. The electrical measurement of noise power will yield the same result in either case and cannot distinguish between them